Use of EB-CFRP to Improve Flexural Capacity of Unbonded Post-Tensioned Concrete Members Exposed to Partially Damaged Strands

Hayder Qays Abbas [1*], Alaa Hussein Al-Zuhairi [1]

[1] Department of Civil Engineering, Faculty of Engineering, University of Baghdad, 10071 Baghdad, Iraq.

Abstract

The study presents the performance of flexural strengthening of concrete members exposed to partially unbonded prestressing with a particular emphasis on the amount (0, 14.2, and 28.5%) of cut strands-symmetrical and asymmetrical damage. In addition to examining the influence of cut strands on the remaining capacity of post-tensioned unbonded members and the effectiveness of carbon fiber reinforced polymer laminates restoration, The investigated results on rectangular members subjected to a four-point static bending load based on the composition of the laminate affected the stress of the CFRP, the failure mode, and flexural strength and deflection are covered in this study. The experimental results revealed that the usage of CFRP laminates has a considerable impact on strand strain. In addition to that, the flexural stiffness of strengthened members becomes increasingly significant within the serviceability phases as the damaged strand ratios increase. The EB-CFRP laminates increased the flexural capacity by approximately 13%, which corresponds to strand damage of 14.28% and about 9.5% for 28.57% of strand damage, which represents one of the unique findings in this field. Additionally, semi-empirical equations for forecasting the actual strain of unbonded tendons were presented. The suggested equations are simple to solve and produce precise results.

Keywords: CFRP Laminate; Debonding; Post-Tensioned Girder; Strand Damage; Unboned Strands.

1. Introduction

Around the world, pre-stressed concrete (PSC) bridges are corroding and falling into disrepair. Recent catastrophic failures have triggered an assessment of the state of numerous pre-stressed structures, resulting in new assignments and, in some cases, issues for emergency deactivation. Several of these collapses and damages are a result of terrorist acts utilizing TNT or rocket attacks, which cause damage to pre-stressed bridge concrete sections or reinforced prestressed tendons. The cutting of strands on concrete members reduces the overall capacity of the structure. Compensation with a carbon fiber-reinforced polymer (CFRP) laminate is one of the ways that this project will try to make things stronger [1]. This study provides an efficient strengthening technique to restore the damaged bridge's girder and to cover the gap of other studies regarding the time-saving of retrofitting the structure and re-entering the service.

CFRP was used to reinforce or retrofit reinforced concrete (RC) or post-tensioned concrete (PC) structures. Reinforced with CFRP laminate is more successful than other conventional methods, such as externally attached steel plates or steel section jacketing. However, because of the appearance of corrosion, it is difficult to work with the weight of steel plates, which adds dead loads to the members. The main sources [2] of damage to bridge members include one

or more of the following: corrosion, degradation, and chloride attack; build-up of fatigue damage; inadvertent damage, such as collision with a vehicle with a higher-than-typical height; tougher assessment rules and improved loading parameters; initial design defects; construction errors; and an absence of maintenance [3]. The additional load-bearing fiber-reinforced polymer can be affixed to increase the capacity of composite materials (CFRP) has come into the strengthening field as a more robust alternative to conventional external reinforcing methods [4].

In the 1980s, Europe and Japan developed the first externally bonded CFRP composite systems for retrofitting concrete members [5]. However, due to the frequent occurrence of bridge incidents, few studies have been conducted on the restoration of collision-damaged girders. Near-surface mounted (NSM) and externally bonded (EB) CFRP composites can be used to reinforce concrete structures (NSM) [6]. The primary concept behind these two systems is to increase the flexural strength and stiffness of the concrete tensile surface by externally connecting CFRP material to it. Although the FRP is applied directly to the member's surface, efficient bonding in any environment requires substantial preparation [7].

Strengthening of RC beams using various promising techniques such as externally bonded steel plates, concrete jacketing, fiber-reinforced laminates or sheets, external prestressing/external bar reinforcement technique, and ultra-high performance concrete overlay has been extensively investigated for the past four decades [8, 9].

The surface on which the attachment is to be applied must be dry, stable, and clean. By ensuring that the compatibility of the strain criteria in the tendons, CFRP reinforcement, and concrete are met, the pre-tensioned tendons help save the integrity of bonded PC members reinforced with FRP tendons [10]. This results in a relatively uniform interaction between both the laminate and the surrounding concrete along with the member [11]. This approach, however, does not exist in un-grooved tendons due to the lack of connection between both the strands and the surrounding concrete. As a result, unbonded strands, adjacent concrete, and FRP laminates interact unevenly along the beam [12]. This could make it less effective for UPC members to strengthen their flexural strength compared to prestressed concrete members with bonded tendons [13]. CFRP composite laminate has been shown to increase the material's bending strength and ability to expand to the elastic zone of PC members. Each FRP application incorporating concrete must be secured with adhesive epoxy [14].

The epoxy class and manner of application are essential aspects of such projects since they might result in premature failure, for example, cover debonding before the target strength is obtained. In comparison to steel reinforcements, it has been demonstrated that FRP composites exhibit a brittle attitude with no or few warning signs preceding failure. However, research has shown that adding CFRP to PS girders can make them much more durable [15].

The failure load of partially prestressed concrete beams with internally unbonded strands was increased by about 2.5%, to 10%, when the jacking stress increased from 0.5 to 0.7 of the strand's ultimate strength. Increasing the concrete compressive strength from 35MPa to 60 MPa led to an increase in load-carrying capacity by about 10% [16].

Carbon fiber reinforced plastic (CFRP) composites are finding huge applications in many industries. Drilling of CFRP composites is required for the assembly of these composite structures in the aerospace industry. This study investigated the feasibility of drilling CFRP composite using a drill bit made of tungsten carbide [17]. Prestressing concrete damage has become a major issue and to improve the ultimate and serviceability, new materials such as carbon fiber reinforced polymers or shape memory alloys can be used for active strengthening [10]. Prestress loss of CFRP during prestressing and service stage is one of the critical technical issues in concrete structures rehabilitation. Eight RC beams strengthened by prestressed CFRP plate were subjected to sustained loading and continuous wetting condition. The results showed that the CFRP end anchorage system had a good long-term performance [18].

This study is a subset of Baghdad University's (Iraq) ongoing investigational research into the effectiveness of strengthening procedures (Civil Engineering Lab). This research focuses on strengthening approaches employing CFRPs with external bonding.

2. Manuscript Scheme

The proposed research involves designing and preparing samples, simulating the impact damage, concrete repairing, CFRP strengthening, static load testing as shown ion Figure 1.
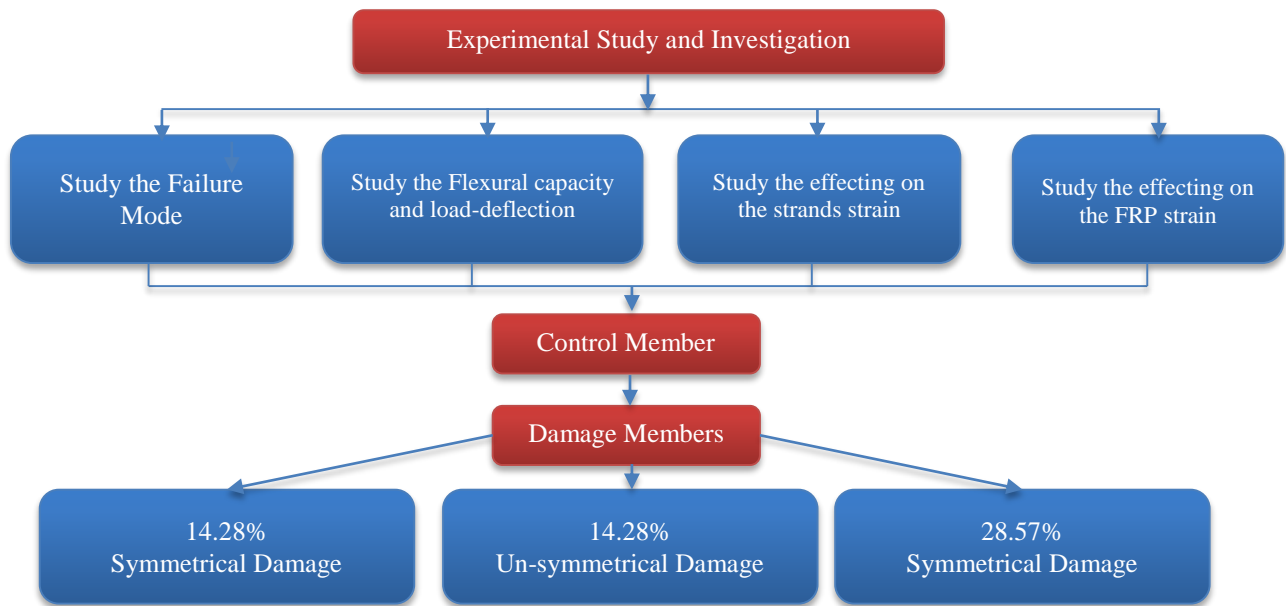
Figure 1. Flowchart for the research methodology

3. Material and Method

3.1. Member Design and Properties

Seven girders, as illustrated in Table 1, have been used in this manuscript, spanning 3000 mm, resting on simply supported ends of 2800 mm apart. The specimen was reinforced with 2f16mm at the bottom and $2\emptyset10$ mm at the top, while the $\emptyset10$ mm bars were used for stirrups. Two unbonded strands are used inside the 22.5mm PVC duct with end grips, and the strand extends to 0.45 meters from each side (Figures 2 and 3). All tests had been done in the laboratory of the college faculty of Baghdad University under four points of loading. CFRP laminates ($b_f = 50$ mm and $t_f = 1.2$ mm) are attached to the soffit to reinforce the specimen, as shown in Figure 4.

Table 1. Summary of specimen testing

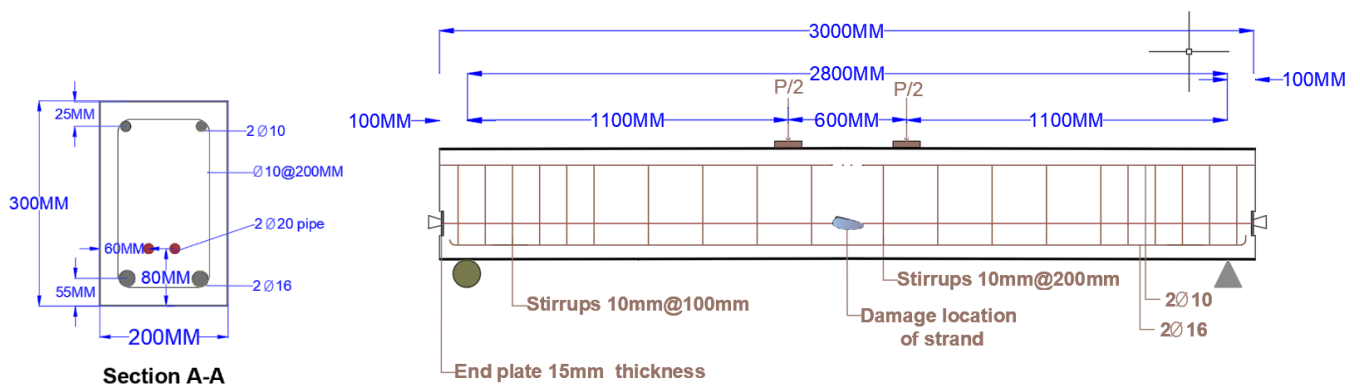| Class	Member ID	Damaged (%)	Symmetrical	Un-symmetrical	Area of a strand (mm²)	CFRP details in (mm)			ρ_p (percent)	ρ_s (percent)
						Thickness	**Width**	**Length**		
Control	REF.	0	—	—	197.40	—	—	—	0.490	
1	B1R	14.28%	●		169.20	—	—	—	0.385	
	B1S					1.20	50.0	2700.0		
2	B2R	14.28%		●	169.20	—	—	—	0.385	0.810
	B2S					1.20	50.0	2700.0		
3	B3R	28.57%	●		141.00	—	—	—	0.320	
	B3S					1.20	50.0	2700.0		

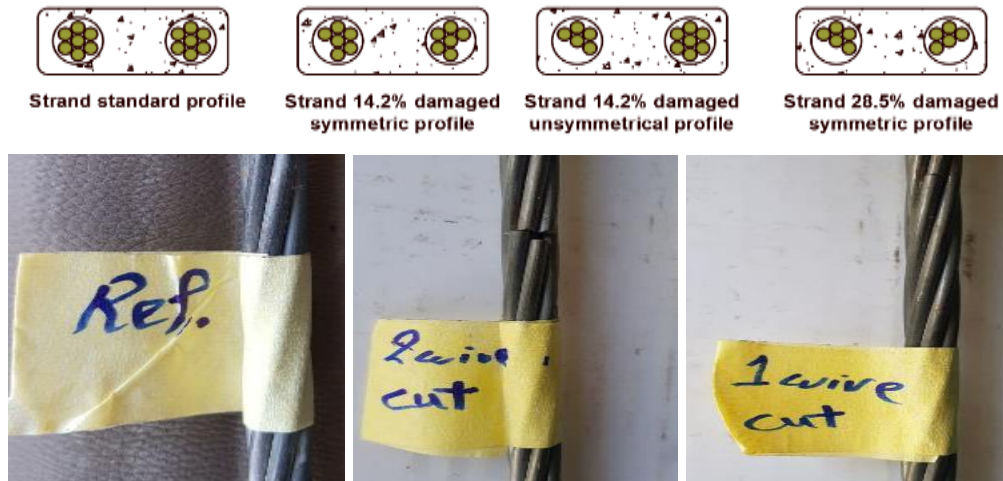**Figure 2. Member's dimension and properties**
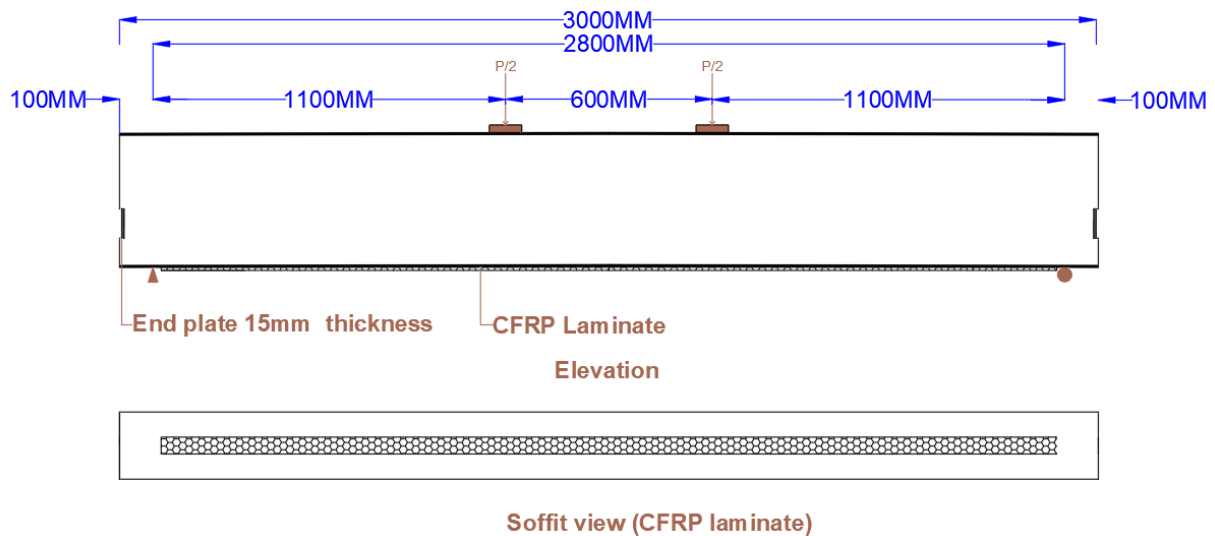
Figure 3. Profile of the damaged strand

Figure 4. Strengthening techniques for this study

The first letter "B" in the specimens' designation stands for beam, and the numbers 1, 2, and 3 after the second letter designate the 14.28 percent and 28.57 percent strands, or damage groups, respectively. "R" for individual group references, and "S" for CFRP laminate strengthening.

The design of the mixture concrete consisted of: Portland cement C45 with 412, 1030, 548, and 245 kg/m^3 for cement, aggregate coarse sand, and fine sand, respectively. (f'c=44.60 N/mm^2 and ft=5.80 N/mm^2) and 5.46 L/m^3 of the superplasticizer. The yield, ultimate, strain and area of bars for steel bars 518.20 N/mm^2, 658.970 N/mm^2, 12.20%, and 77.21 mm^2 respectively for D10 bars and 577.30 N/mm^2, 710.74 N/mm2, 13.40%, and 199.10mm2, respectively for D16 bars (Es=200000 MN/m^2). Nominal area, ultimate strength, yield strength, and ultimate strain were 98.7 mm^2, 1860.00 MN/m^2, 1725.00 MN/m^2, and 5.00% respectively for the Seven wires Garde 270 unboned tendons (Es=197.5 GPa). The manufacturer provided the carbon fiber fabrics' mechanical properties in addition to the resin, in which the nominal thickness, tensile strength, and ultimate elongation were 1.2 mm, 3100 MN/m^2, and 0.02 respectively for laminate (Ef = 170 GPa), and 0.167mm, 3500 MN/m^2, and 1.59% respectively for unidirectional sheet (Ef = 220 GPa).

3.2. Strain Gauges Details and Setup

All members were tested using a unidirectional electrical resistance strain gauge attached at the middle span to measure strain in the strand, FRP, concrete, and steel as the described in Table 2.

Table 2. Properties of strain gauges and location

Type	Code	Ω	Adhesive	QTY, location
Steel	FLAB−6−11	118.5±0.5	CN	2 @ tension bars
Strand	YEFLAB-2-3	119.5±0.5	CN	4
Concrete	PL-60-11	120±0.5	CN-E	1 @ 5cm below the top
CFRP	BFLAB-5-3	119.5±0.5	CN	2

3.3. Instrumentation and Test Procedures

The steel rebar cages were attached with strain gauges of the electric type before being placed in mild steel and wood forms for concrete casting. Using ready-mixed concrete. In addition to the dial gauge for measuring camber, the strain gauge wires were linked to the strain data logger to capture the strain of the strands during the prestressing process. The two 1.5 cm thick end steel plates were fixed at the ends of each specimen with the incision at one of the endplates to protect and guide the strain gauge's wires during the prestressing process. The two endplates were punched with 2.2 cm of diameter for PS ducting. For anchorage at the unbonded strands, two pieces of split-wedge anchor grip (barrel-type) were used. The grips were attached to the far ends of the strands, which were then marked using a permanent pen to determine the level of pre-strain that was applied to each strand. (Δ_L=15.5 cm as per the member design requirement). The first strand was pulled out to the requisite prestressing desired value in two stages: initial for starching the strand and final to the preferred prestressing value. (Δ_L), then released the piston. The procedure was then repeated with the second strand. With pressure gauge readings from the hydraulic jack that is used in the post-tensioning operation as shown in Figure 5.

Figure 5. Operation of post-tensioning

Two of the Analog dial gauges are attached to each end of the strand to find out the slipping of the strand during the loading process. Four LVDTs were used to measure the deflection of the specimens; two near the support, one under the point load, and the last under the quarter-point. All LVDTs were set up to zero strain at the start of testing, as shown in Figure 5. To gradually increase the load, a fifty-ton hydraulic jack was used and attached to the load cell with an ultimate capacity of fifty tons. Increments of 15 kN were added until the cracking load was reached. The load was then applied in 30 kN increments until failure occurred each beam took approximately 2 to 3 hours to complete the test. The load cell was used to monitor the applied load from the frame of the test, in addition to collecting the huge amount of reading data, which lists the load as it was repeatedly applied. Cracks were signified for each load step after the first crack appeared. The fracture pattern on 2 sides of the cross-section was captured on camera after the test. The modes and ultimate loads of failure were reported in each case. During the tests, the load deflection and the first crack, and how it spread were watched (Figure 6).

Figure 6. Member installation on the frame of testing

4. Result and Discussion

The ultimate load-bearing capacity of the member was determined. All reference beams failed in the compression zone due to flexure tensile steel reinforcement yielding.

4.1. Failure Mode

The test girders' performance was measured in terms of maximum load-bearing capability. All of the reference girders failed in the compression zone due to flexure tensile steel reinforcing yielding. While the strengthened beams failed by deboning of laminate followed by sudden compression and tension of concrete and steel bars. The first flexural crack appears in the midspan of sub-reference girders B1R, B2R, and B3R, with cracking loads of the reference girder's cracking load at approximately 94.61, 93.10, and 85.4%, respectively. The cracking propagation is typically shown in Figures 7 and 8. At the end of the test members in the various test series. When the specimens were subjected to the externally applied load, the cracking patterns were most similar and typical of flexural members. All specimens (control and strengthened) grew. During the initial cyclic loading between P_{min} and P_{max}, the first cracks of flexural appear within the constant moment zone.

Figure 7. Failure mode – controlling by debonding

Table 3. Result summary of specimen

Girder ID	Cracking load, in kN	Cracking load concerning the control %	Ultimate Load, kN	Mid-span deflection @ the ultimate load (mm)	Change in flexural strength in compared with control %		Failure mode
B0-control	55.00	———	166.240	26.871	———		SF, CC
B1R	52.00	94.59	157.250	25.470	5.410	R	SF, CC
B1S	62.80	14.11	187.990	24.122	13.080	I	SF, CC-DL
B2R	51.20	93.08	155.2	27.516	6.640	R	SF, CC
B3S	59.10	7.48	193.91	25.123	16.640	I	SF, CC-DL
B2R	47.00	85.41	148.75	29.912	10.540	R	SF, CC
B3S	58.40	6.09	182.42	23.824	9.70	I	SF, CC-DL

SF, steel failure at tension zone, CC crushing of concrete, DL, delamination of CFRP laminate. CD covers delamination, a Negative sign is for reduction, and a positive sign is for increasing. R is for reduction, and I is for increase.

Figure 7, shows the cracking loads Pcr for the individual members before the CFRP application. As a result of the increase in the applied load, the number of cracks increased and began to form within the shear zone. The cracks tended to separate as the load increased to failure and formed more additional flexural cracks. The last column of Table 3; contains a brief of the members' modes of failure. Unbonded PC members failed due to crushing of concrete, CFRP debonding, or a group of these modes. The propagation of interface cracks in the concrete near to the CFRP in a horizontal direction along with the embedded tension rebars until connecting with the vertical flexural cracks caused peeling off of the concrete cover, indicating FRP debonding failure. The control member failed in a more brittle mode than the strengthened members, which was evidenced by more rapid crack propagation and fewer cracks but wider crack widths, while the control girder failed and showed brittle mode while the strengthened girders showed less brittle issue [19], that is explained by propagation fewer and faster cracks with a wide width while a large number of cracks with smaller widths for girders strengthen by carbon fibers.

4.2. Flexural Capacity and Load-Deflection

At three different load levels, the analysis of tested members was investigated: cracking loads, post-cracking elastic stage, and peak loads as shown in Figure 8. The CFRP laminates and tendons had almost no effect on the member attitude when the applied load does not reach the cracking load.
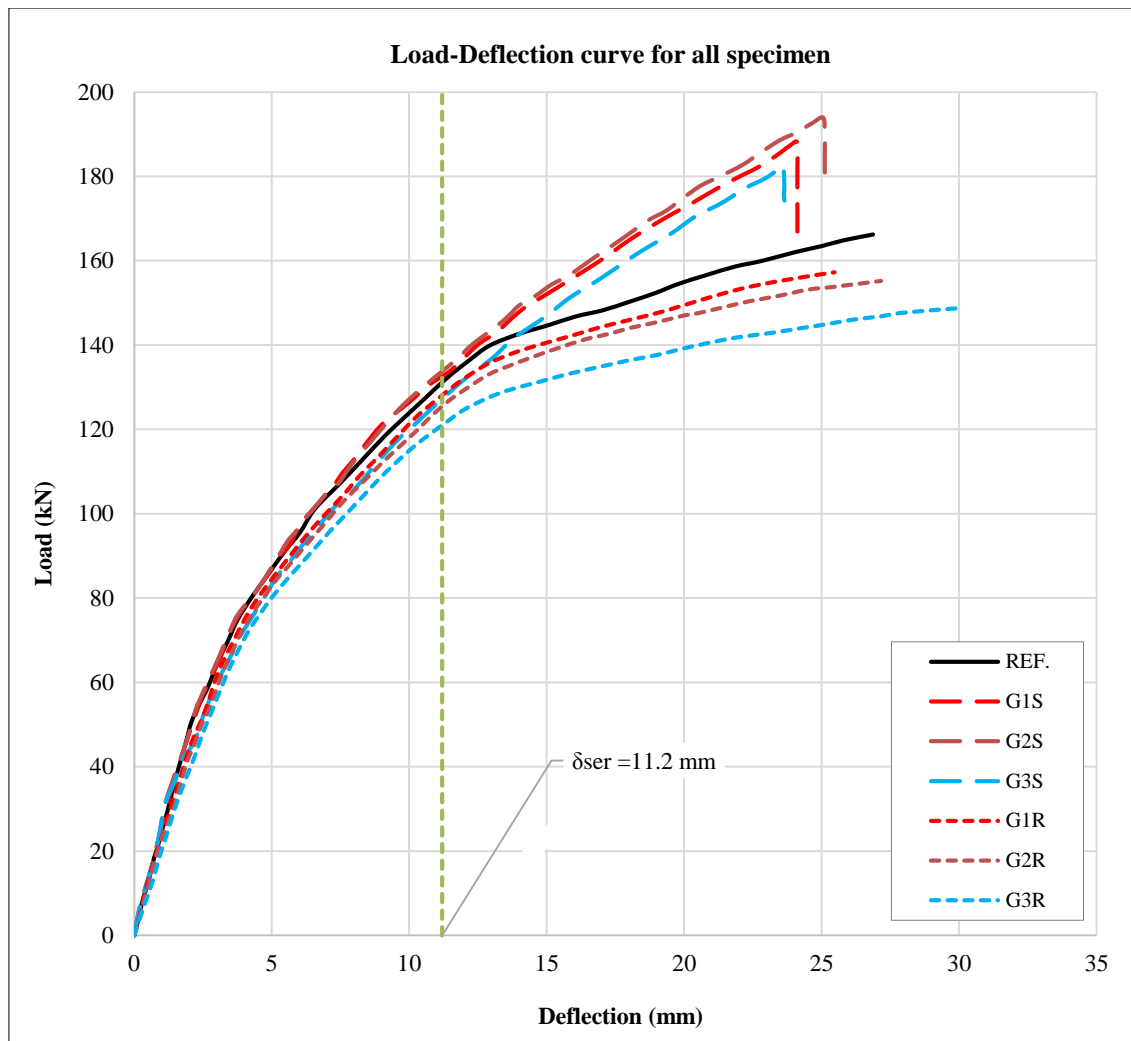
Figure 8. Load verse deflection curves

The findings demonstrate that the damage caused by cutting one and two prestressing strands is significant. (Group 1, 2, and 3) results in a loss of strength when it is compared with the undamaged member; however, the strengthened members with laminated exhibited an increase in flexural capacity of 9-16 percent for groups 1, 2, and 3 as illustrated in Figure 8. The stiffness of the reference girders decreased slightly, and the strengthened girders were not significantly different from the damaged reference girders of the same group. When the applied loads from the frame of testing increase and exceed the cracking load, the damaged members of individual groups exhibit a relatively high rate of stiffness deterioration due to the absence of a portion of the pre-stressing force, which increases the development rate of cracks and displacement. Likewise, the flexural-strengthening externally bonded CFRP of the laminates exhibits their ability to postpone the fracture formation and deterioration of the stiffness of the strengthened girders. As a result, the strengthened member exhibits less deflection than the control girder for the same applied four-point load because of the reduction in the force of prestressing of strands that resist the influence of the applied load.

The deflection is at the same value as the applied load, which is equal to 0.79 from the ultimate load and the ultimate deflection. The serviceability limitation for deflection requirements (span over 250) is considered to use the corresponding value in this manuscript. As per the result of control, the deflection at the serviceability limit is 1.12 cm, and this value is referred to as the permissible load, which is about 79% of the ultimate load. During this period, the displacement of the strengthened girders was slightly reduced by 9–18% for B1S, B2S, and B3S. The maximum displacement increased significantly for the strengthened girders when compared to the controlled girder, which is about 5.3%, 7.51%, and 20.67% for B1S, B2S, and B3S, respectively. CFRP members demonstrate a decrease in displacement at the maximum load, which comes from the obstruction of crack development during loading progression compared with the group references.

4.3. Crack Progression Pattern

Many cracks developed between the two loads in the zone of pure bending moment. As the applied load grew, further cracks occurred outside of this zone, as illustrated in Figure 9.
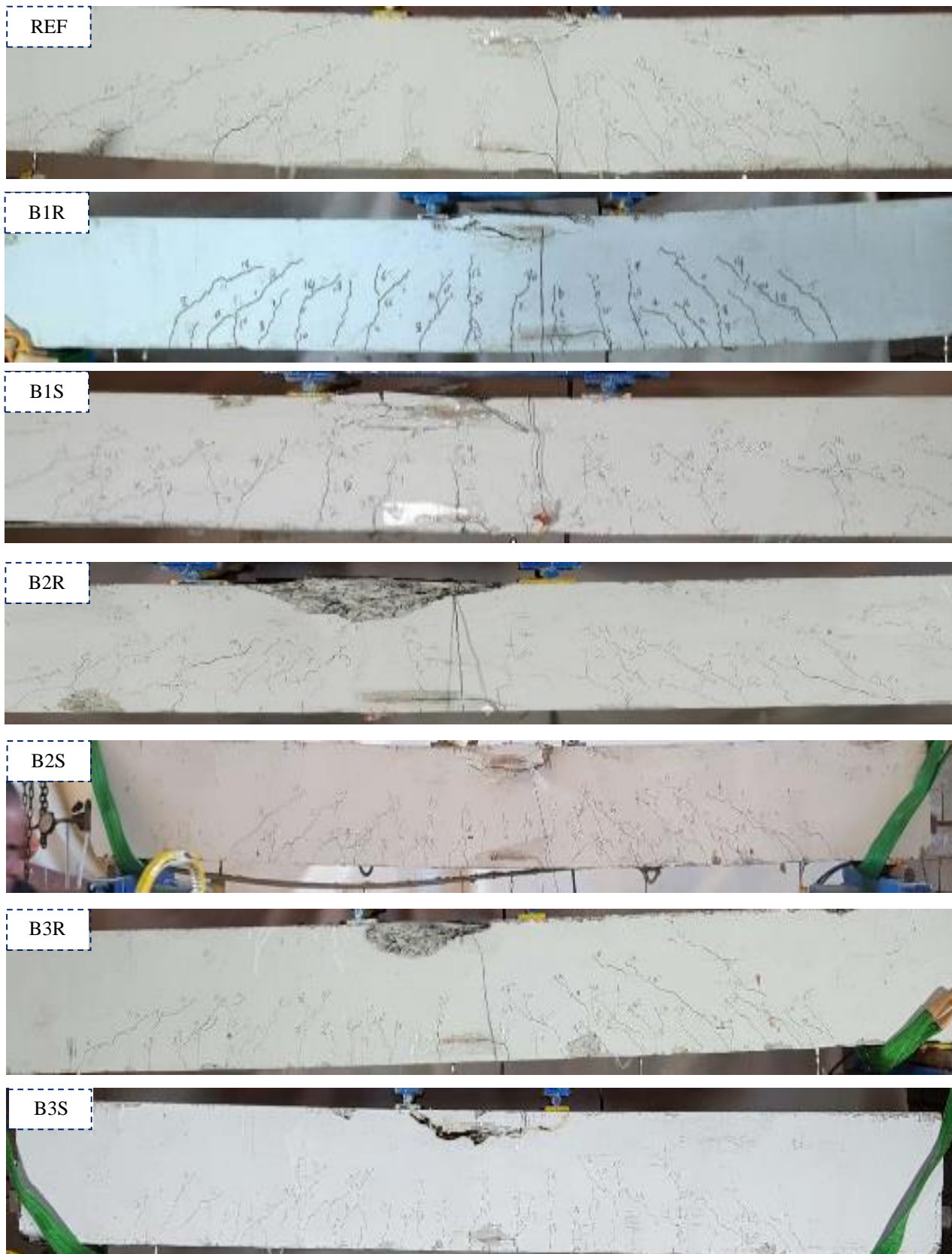
Figure 9. A pattern of cracks at the failure of the tested member

4.4. Applied Load and Strain for the CFRP Laminates

The strain increases in Figure 10 for the CFRP laminates are before the crack load, minimal and nearly equal. After the load reaches the value of the cracking, the strain increases clearly, and after the bonded steel reinforcement yields, the rate of strain increase increases significantly. The increased rates of strain in the carbon fiber reinforced polymer laminates were almost similar.

Load-Strain curve for FRP & Strand-G1

Load-Strain curve for FRP & Strand-G3
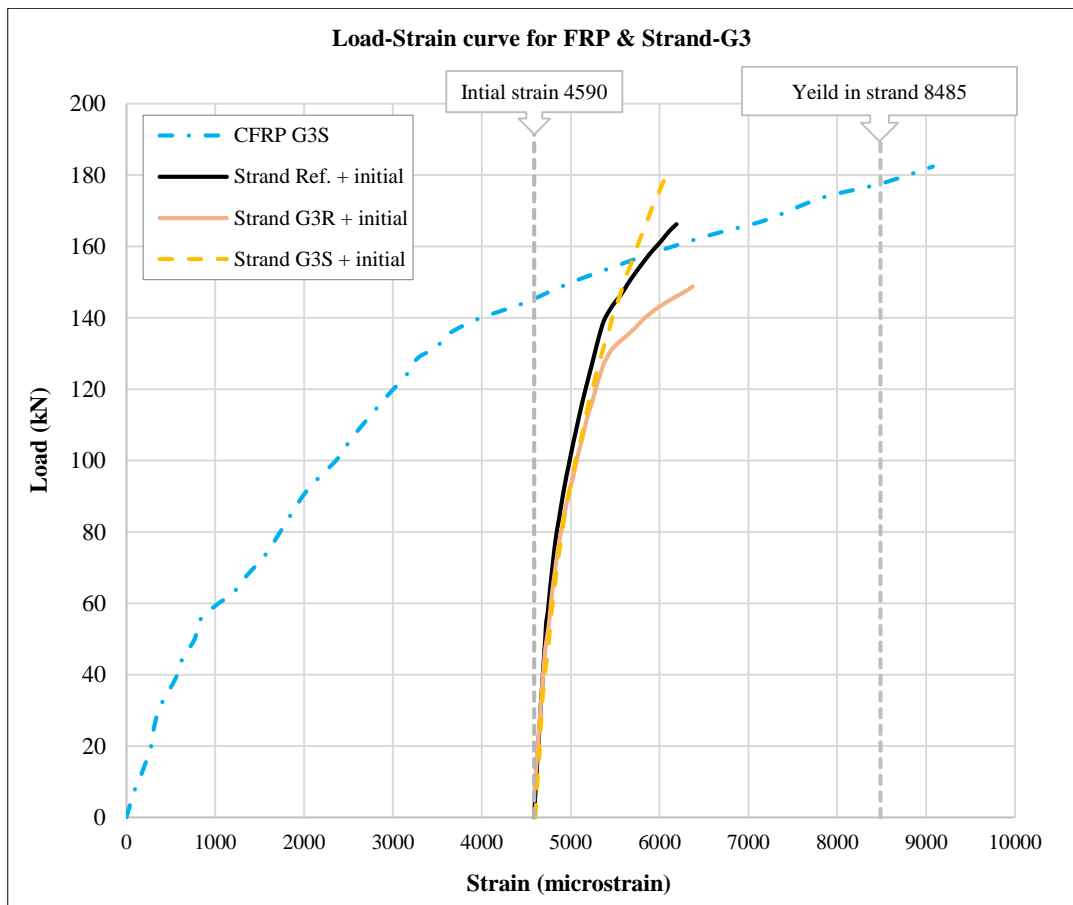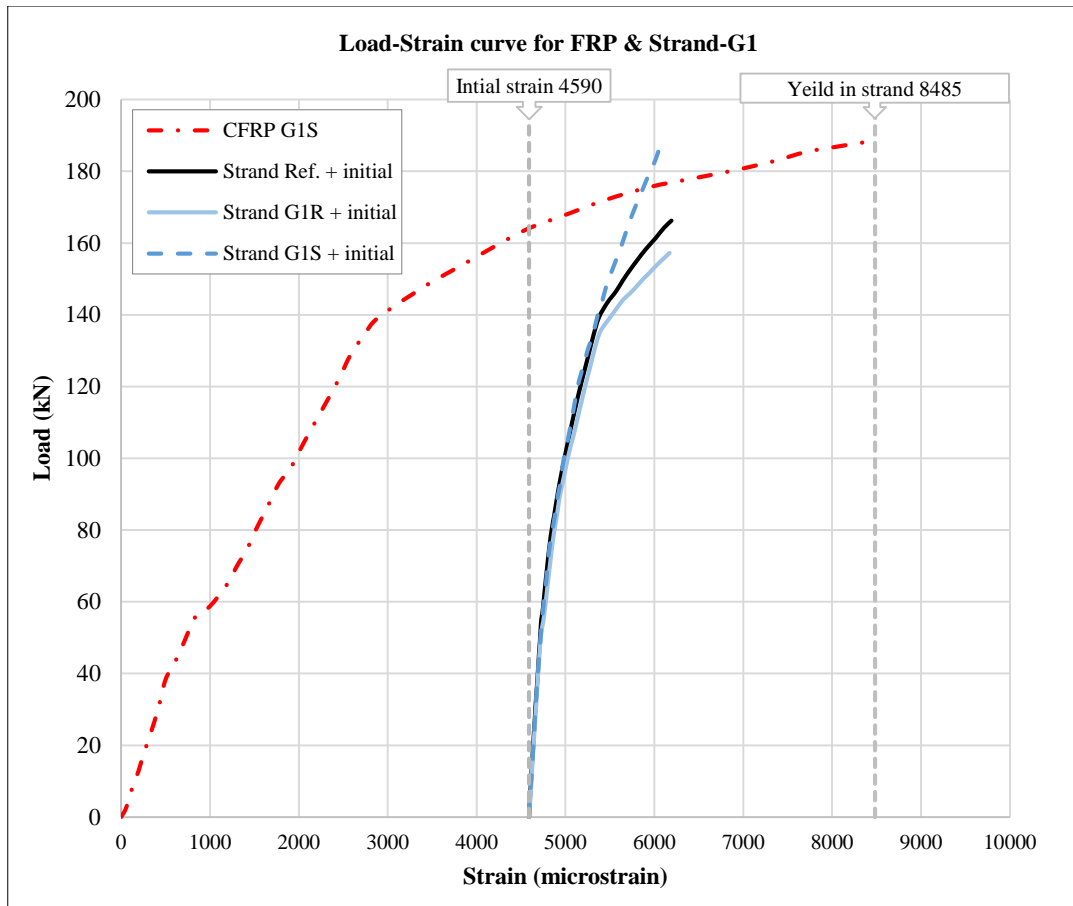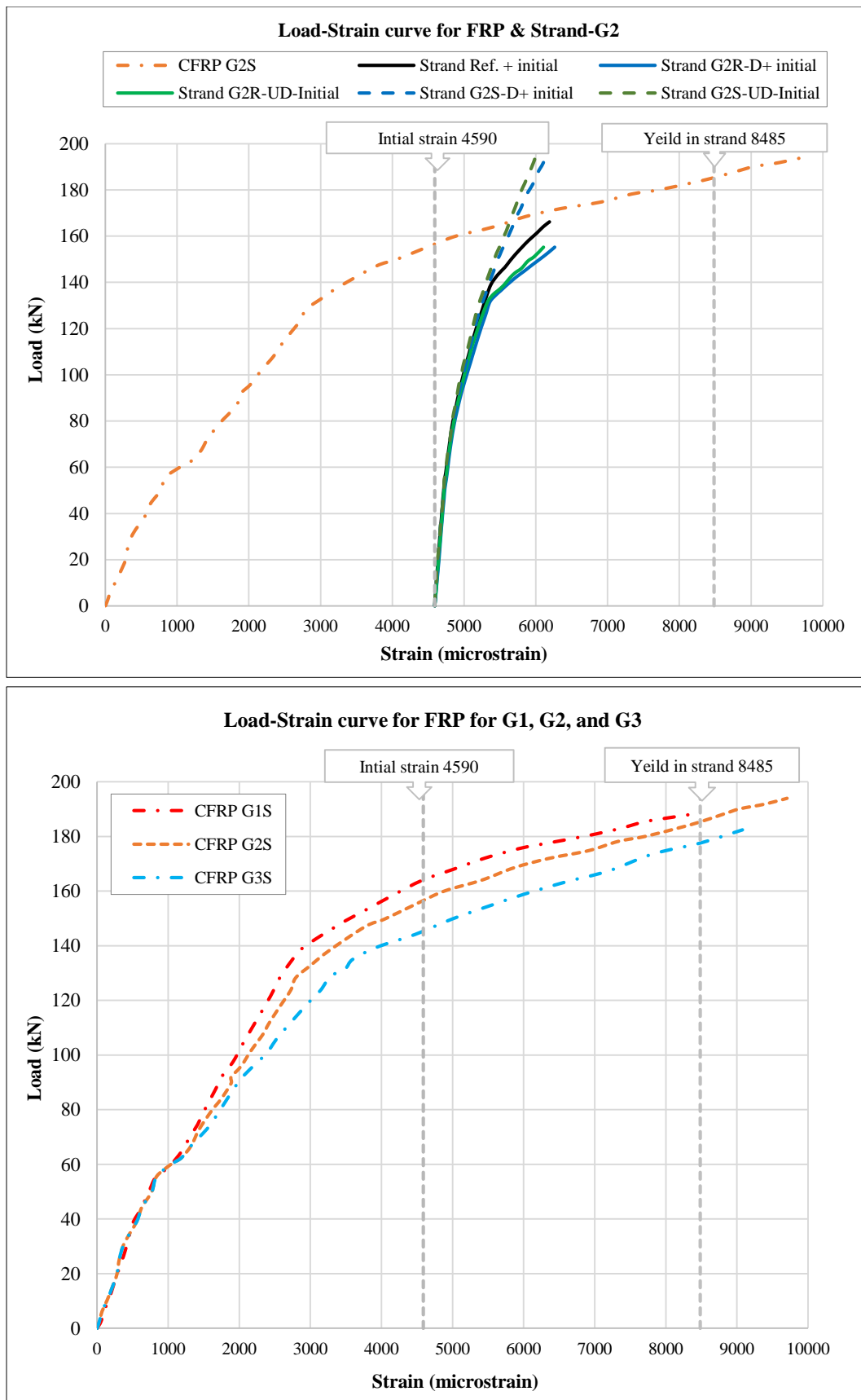
Figure 10. Load-strain for CFRP and strands

At a serviceability load limit, the rise in the strain of strengthened members B1S, B2S, and B3S was 0.265%, 0.294, and 0.346% related to 13.25, 15.42, and 17.3% of the laminate ultimate strain capacity (Fibre Elongation at Break ε_{ffu} = 2%). While the strain increase at the ultimate loads was 0.830 percent, 0.871, and 0.90 percent corresponding to 42.0 percent, 49.1%, and 45.10 percent of the ultimate strain of the fiber capacity for B1S, B2S, and B3S.

4.5. Applied Load and Effecting on the Strands Strain

Because of the minor strain increases, the not contributing of the strand with the flexural strength before the first crack. The increase in the strand strain was calculated by subtracting the post-tensioning initial strain (4600 με,) from the actual strain Figure 10. During this loading stage, the strand acted the same behavior in all of the tested members. The strain increases in the strand for the references groups 1, 2 and 3 were greater than the control girder, whereas the strand strain increases in the members strengthened with laminate was less than the member without strengthening in the same group. At the serviceability load limits, the increase in the strand strain for B1R, B2R, and B3R, was 7500με, 7590με, and 89501με, which showed an increase of about 9 to 30% when compared to the control member. Similarly, the strain increases in the strands of the strengthened girders B1S, B2S, and B3S were 6750 με, 6760 με, and 7620με, with a reduction reaching 15% in comparison with them in parallel in the damaged member references. The strand strain increases were much smaller in the loading stage after the load in the serviceability manner in the strengthened members B1S, B2S, and B3S at the same loading level as in the reference and group reference. As previously mentioned, the carbon fiber laminates were able to delay the cracks and prevent their development and they slowed down the degradation of the member stiffness. Despite significant heterogeneity in the increase in strand strain for members B2R and B2S with unsymmetrical losses in strand area, the average increase in strand strain was comparable to that for members with symmetrical losses in strand area. For example, the coefficient of variation of strand strain increases at the permissible service load was 0.0867 for damage reference beams G1R and G2R, but the COV of the strengthened beams (coefficient of variation) of strand strain increases for B1S and B2S was 0.072.

4.6. Nominal Moment Strength of the UPC

Estimating the bending capacity of prestressed concrete members strengthened with externally bonded carbon fiber laminates necessitates evaluating the strain increase of unbonded prestressed tendons [20]. Unfortunately, design regulations, i.e. only offer a process for estimating the strain increase of bonded prestressed members reinforced with EB-CFRP laminates [20], omitting out the unbonded procedure tendons in members reinforced with Externally Bonded Carbon Fibre Reinforced Polymer laminates. Furthermore, as per the results of the trials, the EB-CFRP laminate has a major effect on the attitude of unbonded tendons. The manuscript assesses the increase in strain for unbonded tendons and bending capacity using the approach given previously [21]. To determine (ε_{ps}) the strain in unbonded strands of the CFRP reinforced simply supported and/or continuous components with nominal flexural strength, the following equation is given:

$$M_n = A_{ps}f_{ps}\left(d_p - \frac{\beta_1 c}{2}\right) + A_s f_s\left(d - \frac{\beta_1 c}{2}\right) + \Psi_f A_f E_f \varepsilon_f\left(d_f - \frac{\beta_1 c}{2}\right), \tag{1}$$

$$fps = F(\varepsilon_{PS}) \tag{1-a}$$

$$fs = E_s \varepsilon_s \le f_y \tag{1-b}$$

$$\varepsilon_{ps} = \varepsilon_{pe} + \varphi_{ps} N_p \varepsilon_c\left(\frac{d_p - c}{L_a}\right). \tag{2}$$

The equation $\varepsilon_{pe} = f_{se}/E_{ps}$ represents the tendon's initial strain, not including stress losses, ε_{pe} (microstrain) which represents the strain of the carbon fiber, E_f (N/mm^2) represents the modulus of elasticity of the carbon fiber, E_{ps} (N/mm^2) which represents the modulus of elasticity of the prestressing strand, f_{se} (N/mm^2) which represents the effective stress of prestressing which is equal to the force over an area (Fp/Ap), F_p (N) which represents the tendon's actual tension force, A_{ps} (mm^2) represents the tendon cross-sectional area, A_f (mm^2) represents the cross-sectional area of carbon fiber = t_{Lf} times b_{Lf}, φ_{ps} which represents the stress reduction factor, set equal to 0.70, φ_f which represents the CFRP reduction factor, set to 0.85 as per [20], and N$_p$ (Unit less factor) which is represent the parameter considered for simply supporting members, Taking $N_P = 14.0$ as a constant [21].

Understanding that stress rarely of the prestressing reinforcement exceeds yield and limiting the related stress to $0.95f_{py}$ allows the use of a linear correlation between prestressing reinforcement strain and stress, that is, $f_{ps} = E_{ps} \times \varepsilon_{ps}$, which results as:

$$f_{ps} = f_{se} + \frac{\varphi_{ps} N_p E_{ps} \varepsilon_c}{L_a/d_p}\left(1 - \frac{c}{d_p}\right) \le 0.95f_{py} \tag{3}$$

The equilibrium compression and tension forces across the rectangular section can be stated as follows, assuming rectangular section action:

$$A_{ps} f_{ps} + A_s f_s + A_f E_f \varepsilon_f = \alpha_1 f_c' b \beta_1 c \tag{4}$$

$$\varepsilon_f = \varepsilon_{cu}\left(\frac{d_f - c}{c}\right) - \varepsilon_{bi} \le \varepsilon_{fd} \tag{5}$$

$$\varepsilon_{fd} = 0.41\sqrt{\frac{f_c'}{n_f E_f t_f}} \le 0.9\varepsilon_{fu} \tag{6}$$

where, ε_{fd} (Micro strain) which represents the debonding strain of the carbon fiber.

Using Equations 2 to 4, to do the step-by-step procedure which can be considered for evaluating the M_n for the nominal moment capacity of carbon fiber reinforced polymer unbonded post-tensioned strengthened members.

Mode I: Concrete Crushing Controlling the Flexural Capacity

Step Number One: Assume that concrete crushing is used to control the nominal flexural strength that is the Equation 5 ≤ Equation 6. For $\alpha_1 = 0.85$, $\varepsilon_c = \varepsilon_{cu}$, and β_1 as defined in [19]. Substituting the f_{ps} from Equation 3 into Equation 4 and the stress reinforcing steel is assumed to be yields which mean $f_s = f_y$. The gained formula is a second-degree equation as listed follow, which is used to calculate the NA depth at nominal flexural strength in the rectangular section under sight:

$$c = \frac{B + \sqrt{B^2 + 4.A.C}}{2.A} \tag{7}$$

with the follow parameter for Equation 7:

$$A = 0.85\beta_1 f_c' b + \frac{\varphi_{ps} N_p A_{PS} E_{ps} \varepsilon_{cu}}{L_a} \tag{7-a}$$

$$B = A_{ps}\left(f_{se} + \frac{\varphi_{ps} N_p E_{ps} \varepsilon_{cu} d_p}{L_a}\right) + A_s f_y - A_f E_f(\varepsilon_{cu} + \varepsilon_{bi}) \tag{7-b}$$

$$C = A_f E_f \varepsilon_{cu} d_f \tag{7-c}$$

Step Number Two: When Equation 5 ≤ Equation 6 as the result. Then calculate the strain in the reinforcing steel ε_s to investigate whether is larger than the yield strain ε_y as assumed in step number 1 Again when Equation 5 ≤ Equation 6 as result, while ε_s is not greater than (ε_y), Now repeat step number One to recalculate more precisely the NA depth by using Equation 7 the following set of quadratic parameters when substituting, is generated.

$$f_s = E_s\left(\varepsilon_s = \varepsilon_{cu} \times \frac{d-c}{c}\right), \tag{8}$$

Instead of $f_s = f_y$ in to Equation:

$$A = 0.85\beta_1 f_c' b + \frac{\varphi_{ps} N_p A_{PS} E_{ps} \varepsilon_{cu}}{L_a} \tag{8-a}$$

$$B = A_{ps}\left(f_{se} + \frac{\varphi_{ps} N_p E_{ps} \varepsilon_{cu} d_p}{L_a}\right) - A_s E_s \varepsilon_{cu} - A_f E_f(\varepsilon_{cu} + \varepsilon_{bi}) \tag{8-b}$$

$$C = A_f E_f \varepsilon_{cu} d_f + A_s E_s \varepsilon_{cu} d \tag{8-c}$$

Step Number Three: Calculate f_{ps} from Equation 3 considering: $\varepsilon_c = \varepsilon_{cu}$, $f_s = E_s \varepsilon_s \leq f_y$. To determine the M_n; nominal moment capacity from Equation 1.

Mode II: FRP Failure Controlling the Flexural Capacity

Step Number Four: When fiber strain ε_f calculated from Equation 5 is greater than debonding strain (ε_{fd}) in Equation 6, which is mean that the CFRP failure occurs just before the strain of concrete (ε_c) in the most distant concrete compression fiber (ε_{cu}). For this matter, the strain in the carbon fiber (ε_f) is equal to debonoding strain ε_{fd}. As a result, a technique of trial-and-error for fulfilling the compatibility of strain and forces equilibrium across the rectangular section's overall height becomes more appropriate, as indicated in the following procedures.

Step Number Five: Using the fiber strain equal to debonding strain ($\varepsilon_f = \varepsilon_{fd}$) as it was assumed initial value of compression zone, evaluate the (ε_c) concrete strain from Equation 9 at the outermost concrete compression fiber, and calculate the gained stress in the prestressing strand from Equation 3 and the gained stress in the reinforcing steel from the Equation 10 by substituting ε_c concrete strain for ε_{cu}.

$$\varepsilon_c = \varepsilon_{fd}\left(\frac{c}{d_f - c}\right) \tag{9}$$

$$f_s = E_s \varepsilon_c\left(\frac{d-c}{c}\right) \tag{10}$$

Step Number Six: Make certain the equilibrium issue by using Equation 4 in which the strain of fiber is equal to the strain of debonding ($\varepsilon_{fd} = \varepsilon_f$), β_1 and α_1 are as calculated from Equations 11 and 12:

$$\beta_1 = \frac{4\varepsilon_c' - \varepsilon_c}{6\varepsilon_c' - 2\varepsilon_c} \tag{11}$$

$$\alpha_1 = \frac{3\varepsilon_c'\varepsilon_c - (\varepsilon_c)^2}{3\beta_1(\varepsilon_c')^2}. \tag{12}$$

where ε_c' can be considered equal to 0.002, which is represent the strain according to f_c' , or for more accurately ε_c' can be calculated as "$\varepsilon_c' = 1.7. \frac{f_c'}{E_c}$.

Step Number Seven: Now steps 5 and 6 must be performed until the force equilibrium requirements of Equation 4 are about equal; if some degree of tolerance is acceptable.

Step Number Eight: Using Equation 1, determine the nominal moment capacity Mn at the section. when "$\varepsilon_f = \varepsilon_{fd}$".

Step Number Nine: For the factored nominal moment is greater than the applied moment ($\varphi M_n \geq M_u$).

Taking into account the reduction factor was determined following the ACI Building code by calculating the correlation between the net tensile strain on the tension reinforcement bars and the NA depth c at nominal flexural strength:

$$\varphi = 0.9 \ for \ {}^c/_{d_e} \leq 0.38 \tag{13-a}$$

$$\varphi = 0.65 \ for \ c/d_e \leq 0.6 \tag{13-b}$$

$$\varphi = 0.65 + 0.25 \left(2.73 - 4.55 \frac{c}{d_e}\right) for \ 0.38 \leq c/d_e \leq 0.6 \tag{13-c}$$

d_e which represents the equivalent depth of the tension reinforcement (FRP laminates, prestressing steel, and reinforcing steel,) and is described as bellows:

$$d_e = \frac{(A_{ps}.f_{ps}.d_p + A_s.f_s.d. + A_f.E_f.\varepsilon_f.d_f)}{A_{ps}.f_{ps} + A_s.f_s + A_f.E_f.\varepsilon_f} \tag{14}$$

As the result, the experimental values of ultimate stress gained unbonded strands were compared to those predicted by the previously given Equation 11. As indicated in Table 4 and Figure 11, the COV for theoretical and practical moments was 0.030.

Table 4. Comparison between the theoretical and experimental moment

| Members for El-Meski & Harajli (2013) [22]				Manuscript data			
Member	Mu-P	Mu-E	Mu-P/Mu-E	Member	Mu-P	Mu-E	Mu-P/Mu-E
UB1_H_F1	41.801	46.501	0.899	Ref	90.090	91.430	0.990
UB1_H_F2	54.302	56.200	0.966	B1R	85.228	86.490	0.990
UB1_P_F1	41.403	46.500	0.890	B2R	85.228	85.360	1.000
UB1_P_F2	55.603	55.810	0.996	B3R	80.525	81.800	0.980
UB2_H_F1	50.502	60.310	0.837	B1S	98.197	103.390	0.950
UB2_H_F2	65.511	70.100	0.935	B2S	98.197	106.650	0.920
UB2_P_F1	58.512	60.500	0.967	B3S	94.374	100.330	0.940
UB2_P_F2	63.303	70.500	0.898	Average "M"			0.966
US1-H-F1	21.400	23.300	0.918	Standard Deviation "SD"			0.029
US1_H_F2	26.900	30.100	0.894	Variation's coefficient "COV"			2.97%
US1_P_F1	21.600	23.800	0.908				
US1_P_F2	30.100	30.800	0.977	For All:			
US2_H_F1	26.600	26.400	1.008	Average "M"			0.968
US2_H_F2	35.800	31.600	1.133	Deviation of standards "SD"			0.079
US2_P_F1	29.800	26.900	1.108	Variation's coefficient "COV"			8.20%
US2_P_F2	37.400	32.100	1.165				
Average "M"			0.969				
Deviation of standards "SD"			0.094	Mu-P is for theoretical (predicated); Mu-E is for experimental			
Variation's coefficient "COV"			9.74%				
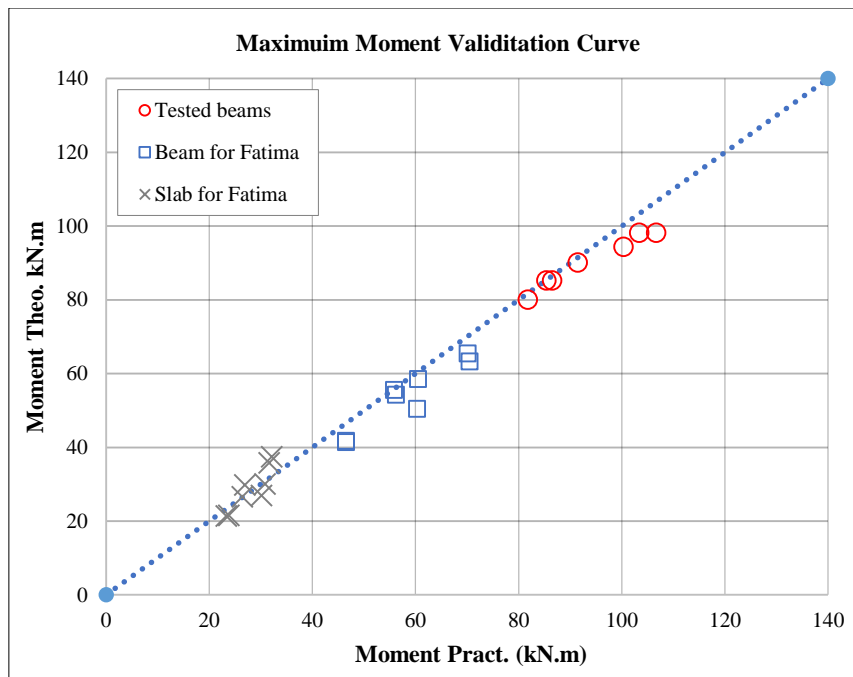
Figure 11. Comparison of experimental and theoretical flexural capacities

5. Conclusions

The impacts of partial strand damage enhanced by externally bonded-carbon fiber-reinforced polymer laminates on post-tensioned concrete members were quantified. The results of the experiments lead to the following conclusions:

- As the ratio of damaged strands grows, the flexural capacity of post-tensioned members diminishes, whereas the displacement of damaged stranded members increases at the same level of loading. At midspan, the damaged strands' flexural capacity is reduced by 5.4%. The capacity of the strengthened specimens is reduced because the strand's strength was lost, and the capacity for strengthened members was increased by 13.08% for B1, 16.64 percent for B2, and 9.73 percent for B3. This means that the capacity is higher than it was before the strand was damaged. Regardless of how much flexural capacity has been restored, it is important to look at the serviceability needs of prestressed concrete members with exceeding 20% losses in strand area before applying any more treatments. The proposed equations for determining strain rises in unbonded post-tension members that are reinforced with externally bonded-CFRP laminates will be very accurate and have very little variance in their estimates of flexural strength (Mean = 0.97 and COV = 8.20%).

- Using externally bonded CFRP laminate methods to control crack development enhances cracking load and flexural capacity. It was a big help when the EB-CFRP laminates were put on unbonded post-tension girders. They made them stronger by 6.0 to 14.0%. The CFRP laminates have a significant effect on the attitude of the strands. At the same loading value, the strain rise in the strands of the CFRP girders was significantly less than that in the damaged beams. And enhancement of bonding for laminate strengthening is a prospect for future research.

6. Declarations

6.1. Author Contributions

H.Q.A. and A.H.A. contributed to the design and implementation of the research, to the analysis of the results and to the writing of the manuscript. All authors have read and agreed to the published version of the manuscript.

6.2. Data Availability Statement

The data presented in this study are available on request from the corresponding author.

6.3. Funding

The authors received no financial support for the research, authorship, and/or publication of this article.

6.4. Conflicts of Interest

The authors declare no conflict of interest.

7. References

[1] Slaitas, J., & Valivonis, J. (2021). Full moment-deflection response and bond stiffness reduction of RC elements strengthened with prestressed FRP materials. Composite Structures, 260, 113265. doi:10.1016/j.compstruct.2020.113265.

[2] Ghaffary, A., & Moustafa, M. A. (2020). Synthesis of repair materials and methods for reinforced concrete and prestressed bridge girders. Materials, 13(18), 4079. doi:10.3390/ma13184079.

[3] Kasan, J. L., Harries, K. A., Miller, R., & Brinkman, R.J. (2014). Limits of Application of Externally Bonded CFRP Repairs for Impact-Damaged Prestressed Concrete Girders. Journal of Composites for Construction, 18(3). doi:10.1061/(asce)cc.1943-5614.0000347.

[4] Aljaafreh, T. (2019). Performance of Precast Concrete Bridge Girders with Externally Bonded Anchored CFRP. Ph.D. Thesis, The University of Texas, Arlington, United States.

[5] Saeed, I. A. (2017). Flexural Performance of Reinforced Concrete Beams Strengthened with Near Surface Mounted Carbon fibre Reinforced Polymer Laminates and Bars under Elevated Temperature. Ph.D. Thesis, Building and Construction Department, University of Technology, Baghdad, Iraq.

[6] Deng, Y., Li, Z., Zhang, H., Corigliano, A., Lam, A. C. C., Hansapinyo, C., & Yan, Z. (2021). Experimental and analytical investigation on flexural behaviour of RC beams strengthened with NSM CFRP prestressed concrete prisms. Composite Structures, 257, 113385. doi:10.1016/j.compstruct.2020.113385.

[7] Kuntal, V. S., Chellapandian, M., Prakash, S. S., & Sharma, A. (2020). Experimental study on the effectiveness of inorganic bonding materials for near-surface mounting shear strengthening of prestressed concrete beams. Fibers, 8(6). doi:10.3390/FIB8060040.

[8] Ganesh, P., & Murthy, A. R. (2019). Repair, retrofitting and rehabilitation techniques for strengthening of reinforced concrete beams - A review. Advances in Concrete Construction, 8(2), 101–117. doi:10.12989/ACC.2019.8.2.101.

[9] Dawood, M. B., & Taher, H. M. A. M. (2021). Various methods for retrofitting prestressed concrete members: A critical review. Periodicals of Engineering and Natural Sciences, 9(2), 657–666. doi:10.21533/pen.v9i2.1849.

[10] Deng, Y., Ma, F., Zhang, H., Wong, S. H. F., Pankaj, P., Zhu, L., Ding, L., & Bahadori-Jahromi, A. (2021). Experimental study on shear performance of RC beams strengthened with NSM CFRP prestressed concrete prisms. Engineering Structures, 235, 112004. doi:10.1016/j.engstruct.2021.112004.

[11] Mohammed, A. M. Y., Ali, A. R. M., & Abdalla, H. A. (2021). Non-linear Behavior of Low Strength RC Beams Strengthened with CFRP Sheets. Civil Engineering Journal, 7(3), 518-530. doi:10.28991/cej-2021-03091670.

[12] Wang, Q., Zhu, H., Zhang, B., Tong, Y., Teng, F., & Su, W. (2020). Anchorage systems for reinforced concrete structures strengthened with fiber-reinforced polymer composites: State-of-the-art review. Journal of Reinforced Plastics and Composites, 39(9–10), 327–344. doi:10.1177/0731684420905010.

[13] Rafeeq, R. (2016). Torsional Strengthening of Reinforced Concrete Beams Using CFRP Composites, Master Thesis, Portland States University, Portland, Unite States.

[14] Chai, H. K., Majeed, A. A., & Allawi, A. A. (2015). Torsional Analysis of Multicell Concrete Box Girders Strengthened with CFRP Using a Modified Softened Truss Model. Journal of Bridge Engineering, 20(8). doi:10.1061/(asce)be.1943-5592.0000621.

[15] Kim, Y. J., Green, M. F., & Fallis, G. J. (2008). Repair of Bridge Girder Damaged by Impact Loads with Prestressed CFRP Sheets. Journal of Bridge Engineering, 13(1), 15–23. doi:10.1061/(asce)1084-0702(2008)13:1(15).

[16] Peera, I., & Oukaili, N. (2021). Experimental Study on the Behaviours of Post-tensioned Concrete Members with Unbonded Tendons. IOP Conference Series: Materials Science and Engineering, 1067(1), 012033. doi:10.1088/1757-899x/1067/1/012033.

[17] Barik, T., Parimita, S., & Pal, K. (2017). Parametric Study and Process Monitoring on Drilling of CFRP Composites. Proceedings of 10th International Conference on Precision, Meso, Micro and Nano Engineering (COPEN 10), 953–957. 7-9 December, Indian Institute of Technology Mardas, Chennai, India.

[18] Li, X., Deng, J., Wang, Y., Xie, Y., Liu, T., & Rashid, K. (2021). RC beams strengthened by prestressed CFRP plate subjected to sustained loading and continuous wetting condition: Time-dependent prestress loss. Construction and Building Materials, 275, 122187. doi:10.1016/j.conbuildmat.2020.122187.

[19] ACI 318-19. (2019). Building Code Requirements for Reinforced Concrete. American Concrete Institute, Farmington Hills, United States. doi:10.14359/51716937.

[20] ACI 440.2R-17. (2017). Guide for the Design and Construction of Externally Bonded FRP Systems for Strengthening Concrete Structure. American Concrete Institute, Farmington Hills, United States.

[21] El-Meski, F. M., & Harajli, M. H. (2013). Flexural Capacity of FRP Strengthened Unbonded Prestressed Concrete Members: Proposed Design Guidelines. 11th International Symposium on Fiber Reinforced Polymer for Reinforced Concrete Structures (FRPRCS-11), 26-28 June 2013, Guimarães, Portugal.

[22] El-Meski, F., & Harajli, M. (2013). Flexural behavior of unbonded posttensioned concrete members strengthened using external FRP composites. Journal of Composites for Construction, 17(2), 197-207. doi:10.1061/(asce)cc.1943-5614.0000330.